FEBS Letters 587 (2013) 272–277

FEBS Letters

journal homepage: www.FEBSLetters.org

Structural studies of cerebral cavernous malformations 2 (CCM2) reveal a folded helical domain at its C-terminus

Oriana S. Fisher [a], Rong Zhang [a], Xiaofeng Li [a], James W. Murphy [a], Borries Demeler [b], Titus J. Boggon [a,*]

[a] Department of Pharmacology, Yale University School of Medicine, 333 Cedar Street, New Haven, CT 06520, United States
[b] Department of Biochemistry, The University of Texas Health Science Center at San Antonio, San Antonio, TX 78229, United States

ARTICLE INFO

Article history:
Received 29 September 2012
Revised 26 November 2012
Accepted 11 December 2012
Available online 22 December 2012

Edited by Christian Griesinger

Keywords:
Protein–protein interaction
Signal transduction
Cerebral cavernous malformation
X-ray crystallography
Harmonin-homology domain

ABSTRACT

Cerebral cavernous malformations (CCM) are neurovascular dysplasias affecting up to 0.5% of the population. Mutations in the *CCM2* gene are associated with acquisition of CCM. We identify a previously uncharacterized domain at the C-terminus of CCM2 and determine its 1.9 Å resolution crystal structure. Because this domain is structurally homologous to the N-terminal domain of harmonin, we name it the CCM2 harmonin-homology domain or HHD. CCM2 HHD is observed in two conformations, and we employ analytical ultracentrifugation to test its oligomerization. Additionally, CCM2 HHD contains an unusually long 13-residue 3_{10} helix. This study provides the first structural characterization of CCM2.

Structured summary of protein interactions:
CCM2 binds to **CCM3** by pull down (View interaction)
CCM2 and **CCM2** bind by X-ray crystallography (View interaction)
CCM2 and **CCM2** bind by molecular sieving (View interaction)

1. Introduction

Cerebral cavernous malformations (CCM) are neurovascular dysplasias that occur in up to 0.5% of the population [1]. Both the familial and sporadic forms of the disease most commonly result in the formation of hemorrhage-prone lesions in the brain [1] that are associated with stroke, seizure, or other neurological sequelae [1]. Approximately 20% of familial cases of CCM are associated with autosomal dominant inheritance of mutations in the gene CCM2 (*malcavernin*; *osmosensing scaffold for MEKK3*, *OSM*) [1]. The formation of lesions is thought to be associated with a 'second-hit' somatic mutation resulting in complete loss of functional CCM2 [2,3]. CCM2 is also essential for embryonic angiogenesis, and its endothelial-specific loss is lethal mid-gestation [4,5]. The molecular and structural underpinnings of CCM2 function are therefore of significant cell biological and clinical interest.

CCM2 is a 444 amino acid protein predicted to contain a phosphotyrosine binding (PTB) domain at its N-terminus [6]. It is thought to interact directly with both KRIT1 (Krev interaction trapped-1; CCM1) and CCM3 (programmed cell death 10; PDCD10) to form the CCM complex [7]. The CCM2 PTB domain interacts with KRIT1 via conserved NPxY/F motifs in the KRIT1 N-terminus [8]. CCM2 also directly interacts with CCM3, but the interaction interface is not well characterized [7,9]. CCM2 is therefore the hub of the CCM complex, scaffolding to both KRIT1 and CCM3. CCM2 has also been implicated as an osmosensitive scaffold for p38 MAP kinase cascades [10,11] and in degradation of the GTPase RhoA [5,12].

The C-terminal portion of CCM2 has not been well described. This approximately 200 amino acid region cannot be homology modeled to known protein domains [13]. It is not yet known whether the CCM2 C-terminus contains a folded domain, nor how that domain may function in the cell. The C-terminus does, however, appear to be capable of inducing cell death through a pathway involving the neurotrophin receptor TrkA [13]. The molecular basis for this requirement is not understood.

In this study, we provide the first molecular level analysis and crystal structure of the C-terminus of CCM2. We find a helical domain that bears distinct structural similarity to the N-terminal domain of the Usher syndrome scaffolding protein harmonin [14,15] that we find can exist in two distinct conformational states.

2. Materials and methods

2.1. Protein expression and purification

Four human CCM2 (UniProt ID: Q9BSQ5) constructs were subcloned into a modified pET32 vector with a TEV-cleavable N-termi-

* Corresponding author. Address: Department of Pharmacology, Yale University School of Medicine, SHM B-316A, 333 Cedar Street, New Haven, CT 06520, United States. Fax: +1 203 785 5494.
E-mail address: titus.boggon@yale.edu (T.J. Boggon).

0014-5793/$36.00
http://dx.doi.org/10.1016/j.febslet.2012.12.011

nal hexahistidine (6xHis) tag: CCM2-FL (residues 1–438), CCM2-CT (residues 231–438), CCM2-CT3 (residues 283–438) and CCM2-HHD (residues 283–379). These were expressed in *Escherichia coli* Rosetta (DE3) cells (Novagen) and purified (Supplementary data).

2.2. Limited proteolysis

Limited proteolysis was performed on CCM2-FL and CCM2-CT as described in Supplementary data.

2.3. Crystallization and structure solution of CCM2 C-terminal domain

Optimized CCM2-HHD crystals were obtained with precipitant conditions of 2.072 M ammonium sulfate and 0.2 M potassium formate (Supplementary data). Because CCM2-HHD has no discernable homology to other determined protein structures by sequence alignment, we determined the structure by the single-wavelength anomalous diffraction (SAD) method using an osmium derivative (Supplementary data). The structure is deposited in the PDB with accession code 4FQN.

2.4. Light scattering and analytical ultracentrifugation

SEC-MALS was performed on purified CCM2-HHD or CCM2-HHD-E290R concentrated to 1 mg/ml. Data analysis was performed using ASTRA 6 software (Wyatt Technology). Sedimentation velocity experiments were performed to monitor possible mass action in the oligomerization behavior of CCM2. Both wild-type and CCM2-HHD-E290R were measured over 13–224 μM for the wild-type and 11–239 μM for CCM2-HHD-E290R (Supplementary data).

3. Results

3.1. CCM2 contains a C-terminal domain

The CCM2 protein contains an N-terminal flexible loop of approximately 60 residues, a predicted PTB domain (encoded approximately by residues 60–220) [6], and a C-terminal region (residues ~220–444) (Fig. 1A). No sequence homology to structural domains has previously been detected in the C-terminal region of CCM2, although it has been suggested to play a role in promoting apoptotic signaling by the TrkA receptor tyrosine kinase [13] and has predicted secondary structure. To identify whether a folded domain exists at the CCM2 C-terminus, we conducted limited proteolysis on full-length CCM2 (CCM2-FL) by incubating it with serial dilutions of three different proteases. A species of approximately 21 kDa molecular mass was present after treatment with all three proteases (Fig. 1B) that N-terminal sequencing identified to begin at A232. This is slightly downstream from the predicted PTB domain, indicating the presence of a proteolytically stable C-terminal region of CCM2. Therefore, we produced a CCM2 construct encompassing residues R231–S438 (CCM2-CT) that we found by circular dichroism analysis to contain approximately 40% helical and 10% strand content, suggesting that the C-terminus of CCM2 can independently fold as a stable domain. Because this region of the protein was recalcitrant to crystallization, however, we conducted a second limited proteolysis analysis (Fig. 1C). This yielded another region (CCM2-CT2) of approximately 17 kDa molecular mass that N-terminal sequencing determined to start at C269. Taking into account the limited proteolysis results and secondary structure predictions, we designed two further CCM2 constructs encompassing residues S283–S438 (CCM2-CT3) and residues S283–G379 (CCM2-HHD). This analysis provides direct experimental evidence in support of a folded domain at the C-terminus of CCM2 (Fig. 1A).

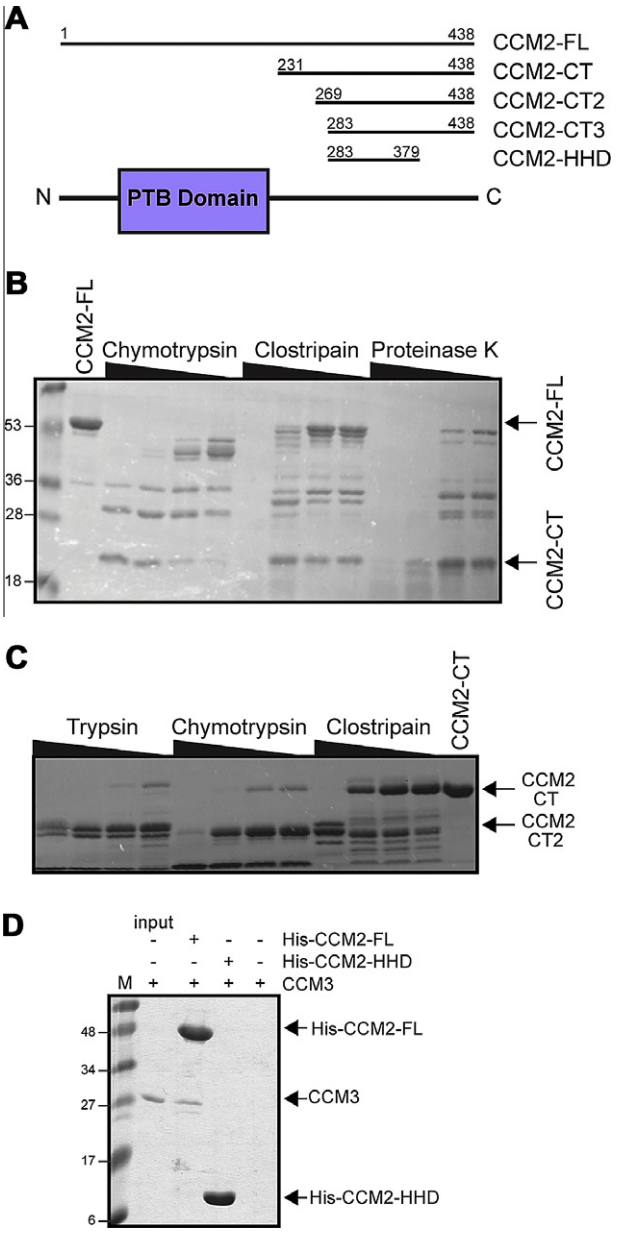

Fig. 1. Domain organization of CCM2. (A) Domain schematic of CCM2. The predicted PTB domain is shown in purple and the C-terminal regions identified in this study are indicated; (B) limited proteolysis of full-length CCM2 (CCM2-FL) using a serial dilution of proteases reveals a proteolytically resistant portion of CCM2 (CCM2-CT); (C) limited proteolysis using CCM2-CT as input identifies a second proteolytically resistant region (CCM2-CT2); (D) pull-down assay. CCM2-FL or CCM2-HHD were bound to nickel-beads and incubated with CCM3. Right hand lane is CCM3 pull-down by empty beads.

3.2. The CCM2 C-terminal domain does not interact with CCM3

CCM2 has been shown to interact with another cerebral cavernous malformation-associated protein, CCM3 [7,9], through a small region C-terminal to the predicted PTB domain potentially corresponding to residues 220–245 [16]. Indeed, purified constructs including this region can bind CCM3 [9]. To confirm that the newly identified C-terminal domain of CCM2 does not bind CCM3, we conducted pull-down experiments using immobilized CCM2-FL or CCM2-HHD with purified CCM3 as input. We observed that while CCM2-FL pulls down CCM3, CCM2-HHD does not (Fig. 1D).

3.3. Overall structure of the CCM2 C-terminal domain

The proteolytically resistant C-terminal domain of CCM2 has low primary sequence similarity to previously determined structures, suggesting that it may comprise a novel fold. We therefore determined its structure by X-ray crystallography by using the SAD method (Fig. S1), and refined against a 1.9 Å native dataset (Table S1). Overall, we found good electron density throughout the structure (Fig. S1), with four copies of CCM2 per asymmetric unit. The CCM2 C-terminus folds as a globular domain comprised of a five-helical bundle that we denote as helices H1 to H5 with a 4-residue helix (H1*) present at the N-terminus of chains A and B. Although helices H1, H2, H3, H5, and H1* are α-helices, helix H4 is a long 13-residue 3_{10} helix (Fig. 2A and B). A 3_{10} helix of this length is uncommon, as the majority of 3_{10} helices observed in protein structures are typically only 3 or 4 residues [17]. Occasionally, however, helices of comparable length are found, as discussed in a 2006 survey of 3_{10} helices in the Protein Data Bank [17] that cited a 15 residue helix in PDB 1PZ4 [18]. The low frequency of longer 3_{10} helices is likely due to decreased structural stability, resulting in more stringent packing requirements [19]. The 3_{10} helix of CCM2 packs against helices H1 and H5 and is anchored by two salt bridges at its N- and C-termini made by residues R346 and R354 binding helix H1 residue E314 and helix H5 residue E366, respectively. The conserved P355–F356 pair at the C-terminus of H4 is also potentially important for stabilizing this helix (Fig. 2C). The overall structure of CCM2-HHD encompasses residues S283–K375.

3.4. The CCM2 C-terminal domain is homologous to the N-terminal domain of harmonin

To investigate whether the C-terminal domain of CCM2 folds in a similar fashion to previously determined structures, we submitted each of the four chains to the Dali server. We found that there is distinct structural similarity to the Usher syndrome scaffolding protein harmonin (PDB IDs: 3K1R, 2KBQ, 2KBR) [14,15], a protein involved in mechanotransduction in hair cell bundles (Fig. 2D). Although sequence identity between the CCM2 C-terminal domain and the harmonin N-terminal domain is only 14% over 80 residues (Fig. 2E), the Dali server yielded *Z*-scores between CCM2 and harmonin that ranged from 8.6 to 11.9 and root-mean-square deviations (RMSD) from 1.7 to 2.6 Å over 71–80 C_α atoms. Based on this structural similarity, we therefore denote this domain in CCM2 the harmonin-homology domain, or HHD.

3.5. The CCM2 HHD crystal structure indicates two conformational states

The CCM2 HHD crystallizes with four copies per asymmetric unit. Analysis of the crystal packing reveals two distinct conformations. Two of the copies (chains A and B) have an extensive interaction interface between them (Fig. 3A), but this interface is not observed for the other two copies (chains C and D) either in the asymmetric unit or with symmetry-related molecules. Chains A and B are experimentally identical (RMSD is 0.55 Å over 93 C_α [20]) and chains C and D are structurally very similar (RMSD is 0.75 Å over 76 C_α). The two classes (A/B and C/D), however, are conformationally more divergent from one another (e.g., the RMSD between chains A and D is 1.39 Å over 76 C_α). This divergence is centered on the N-terminal portion of the CCM2 HHD up to residue S311 (RMSD for residues 311–375 between chains A and D is 0.87 Å over 65 C_α) (Fig. 3B). Although there is strong electron density for residues S283–S311 in both chains A and B, this N-terminal region is partly disordered in chains C and D, for which S292 and L299 are the first visible residues, respectively. Furthermore, in the visible N-terminal portions of chains C and D, helix H1 is

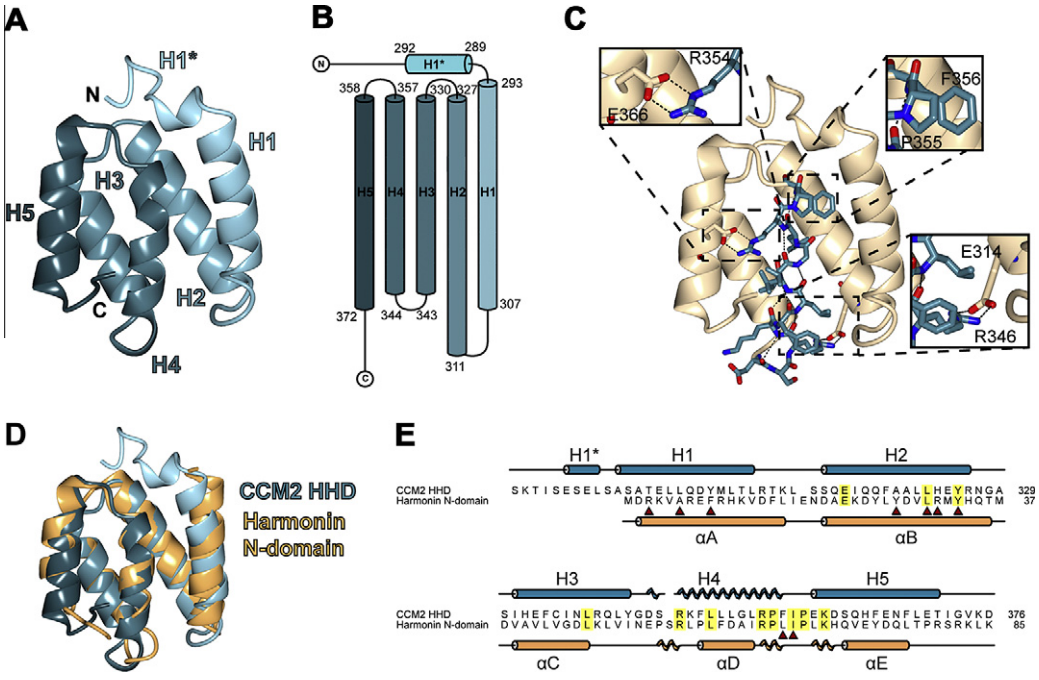

Fig. 2. Overall structure of CCM2 harmonin-homology domain (HHD). (A) cartoon diagram of the CCM2 HHD (chain A) with helices labeled. Structural images generated using CCP4MG [20]; (B) topology diagram of the CCM2 HHD generated using TopDraw; (C) cartoon diagram of CCM2 with the 3_{10} helix (H4) highlighted in teal. Insets show regions that stabilize the 3_{10} helix: a salt bridge between R354 and E346 (upper left), a salt bridge between R346 and E314 (lower right), and conserved residues P355 and F356 (upper right); (D) superposition of the N-domain of harmonin (PDB ID: 3K1R) [14] in orange and the CCM2 HHD in teal; (E) structure-based alignment of CCM2 HHD to the harmonin N-domain generated using Aline. The secondary structure of CCM2 is depicted above its sequence and the secondary structure of harmonin below its sequence. α-helices are shown as cylinders and 3_{10} helices as spirals. Residues highlighted in yellow are conserved between CCM2 and harmonin. Red triangles denote harmonin residues that bind cadherin 23.

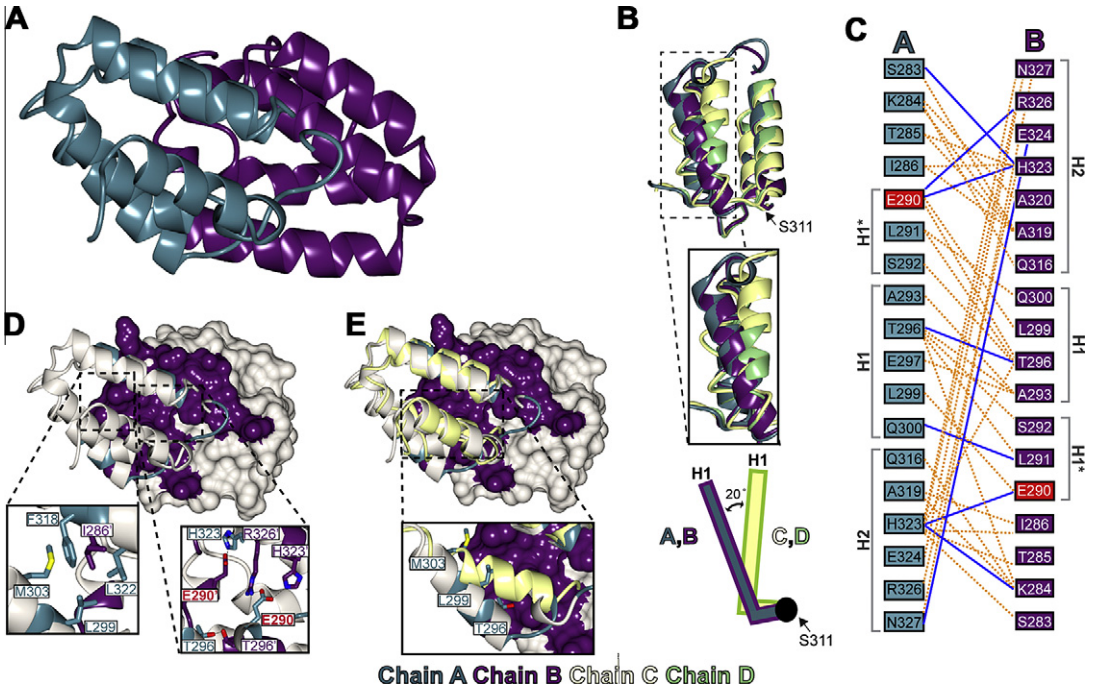

Fig. 3. The CCM2 harmonin-homology domain putative dimerization interface. (A) Crystallographically observed interaction interface between CCM2 HHD chains A and B. Chain A is colored in teal and chain B in purple; (B) superposition of the four molecules in the ASU. Chain A is colored in teal, B in purple, C in yellow, and D in green. The hinge residue S311 is indicated by an arrow. Inset shows the two conformations of helix H1. Schematic illustrates the conformational change in helix H1; (C) map of residues involved in the CCM2 HHD interface. Residue E290 is mutated in this study and indicated in red; (D) chain B shown in surface view and A as a ribbon diagram. Residues involved in mediating the interface are depicted in purple or teal for chain B or A respectively. Insets are close-ups of key residues involved in the hydrophobic pocket (left) and charge cluster (right); (E) superposition of chain C (yellow) on chain A, with chain B shown as a surface. The two CCM2 HHD conformations are incompatible with each other.

conformationally hinged closer to the hydrophobic core of CCM2 HHD by approximately 20° (by HELIXANG) and pivots around residue S311 (Fig. 3B).

3.6. Structural analysis of the interface between chains A and B

The crystallographically observed interface between chains A and B encompasses 18 residues from each chain, and comprises 9 hydrogen bonds and 109 non-bonded contacts (as defined by PDBSum) (Fig. 3C). The interface between molecules A and B buries a total surface area of 1911 Å^2 (956.9 Å^2 from chain A and 954.1 Å^2 from chain B) as defined by the PISA server and has a shape complementarity of 0.64 [21] (Fig. 3D). The PISA server also shows this interface to have a Complex Formation Significance Score (CSS), a measure of interface relevance, of 1.000. The interaction is almost twofold symmetric and encompasses the N-terminus through residue Q300 and residues Q316–N327. This includes helix H1*, the N-terminal portion of helix H1, and the C-terminal portion of helix H2. The interaction surface is predominantly comprised of three regions: two hydrophobic pockets and a charge cluster. Because of the almost twofold symmetry, the charge cluster is found at the center of the interface and the hydrophobic pockets on the edge (Fig. 3E) (Supplementary data).

3.7. Determination of the oligomeric state of the CCM2 HHD by size exclusion chromatography with light scattering and analytical ultracentrifugation

Because of the presence of both monomeric and dimeric forms of the CCM2 HHD in the crystal structure and the fact that the dimeric interface is evolutionarily conserved (Fig. S2), we tested the oligomeric state of the CCM2 HHD by size exclusion chromatography coupled with multi-angle light scattering (SEC-MALS). We found that both dimeric and monomeric forms of CCM2-HHD are present in solution as determined by SEC-MALS, with the monomeric species making up the majority of the protein (Fig. 4A). We also confirmed that the dimeric peak was CCM2-HHD by N-terminal sequencing and that dimerization was not due to disulfide formation by analysis of non-reducing SDS–PAGE (data not shown). We next generated a point mutation at the dimer interface, E290R, and found by SEC-MALS that the small dimeric peak was no longer observed (Fig. 4B).

Since our light scattering data neither completely rule out the existence of a CCM2-HHD dimer nor fully validate it, we next sought to study the dimerization equilibrium of the putative dimer by analytical ultracentrifugation (AUC). Sedimentation velocity experiments (SV) were carried out to determine the oligmeric state of CCM2-HHD and CCM2-HHD-E290R. We examined both wild-type and mutant over a range of loading concentrations to determine any possible mass action effects (Table S2). These experiments showed homogeneous compositions for both wild-type and mutant (Fig. 4C), resulting in molecular weights consistent only with a monomer of CCM2-HHD (Fig. 4D). Sedimentation profiles from multiple loading concentrations did not produce any change in the sedimentation behavior, suggesting the absence of any mass action. Both wild-type and mutant displayed essentially identical sedimentation coefficients at all investigated concentrations. While the sedimentation resulted in observations of monomeric protein, these experiments were carried out at concentrations substantially lower than the crystallization experiments. These results do not preclude a monomer–dimer affinity in the concentration range present during crystallizations. However, AUC experiments conducted at such high concentrations may be problematic.

Together, the SEC-MALS and AUC results suggest that the homodimer observed in the crystal structure may represent a weak

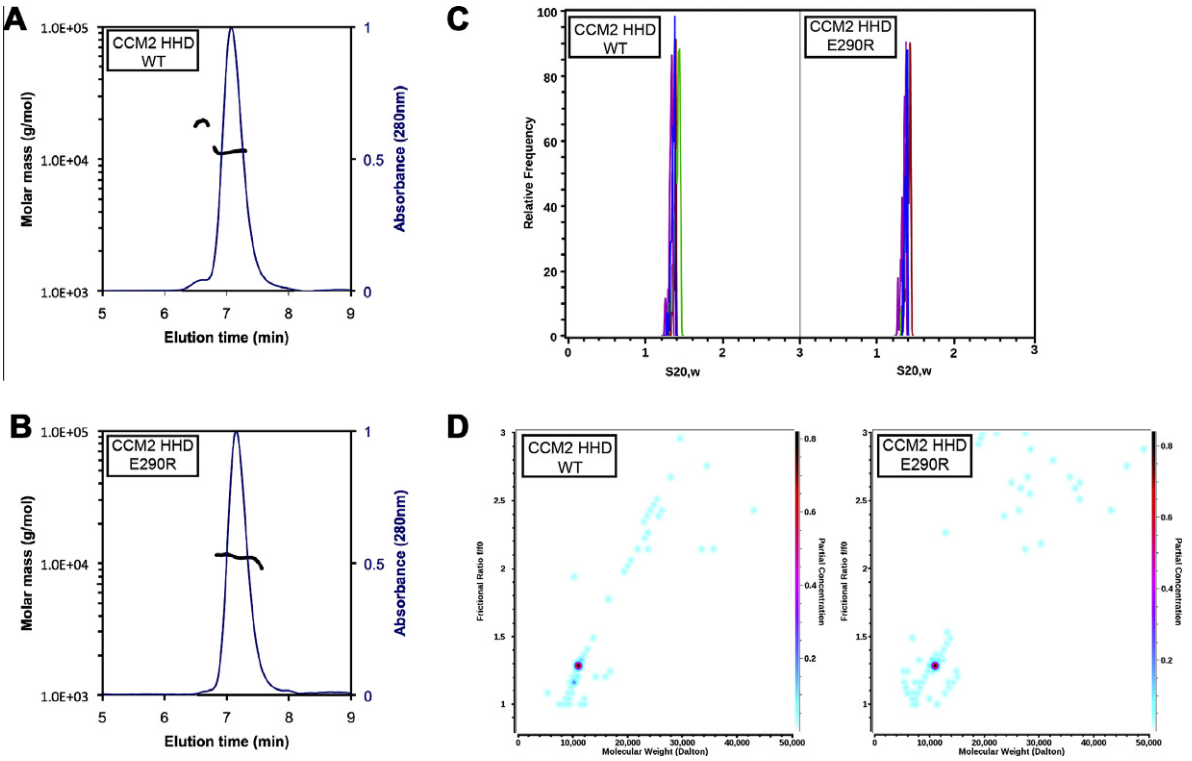

Fig. 4. Size exclusion chromatography with multi-angle light scattering (SEC-MALS) and analytical ultracentrifugation (AUC) analysis of CCM2 HHD. (A) SEC-MALS analysis of the 11.1 kDa CCM2-HHD. Two peaks are observed: a monomeric peak with a molecular weight of 11.1 kDa ±2% and a dimeric peak with a molecular weight of 19 kDa ±2%. Molar mass is plotted on the primary *y*-axis, and normalized A_{280} on the secondary *y*-axis; (B) SEC-MALS analysis of CCM2-HHD-E290R. One peak is observed, with molecular weight of 11.1 kDa ±1.4%; (C) van Holde–Weischet sedimentation coefficient distributions for CCM2-HHD (left), measured at 0.59 OD_{230} (red), 1.14 OD_{230} (green), 0.4 OD_{280} (magenta), and 1.0 OD_{280} (blue), and CCM2-HHD-E290R (right), measured at 0.49 OD_{230} (red), 1.1 OD_{230} (green), 0.37 OD_{280} (magenta), and 1.07 OD_{280} (blue). The narrow sedimentation distribution of both CCM2-HHD and CCM2-HHD-E290R forms indicates homogeneity, and suggests that all concentrations reflect the same oligomeric state; (D) 2-dimensional spectrum analysis fit combined with a 50 iteration Monte Carlo analysis. CCM2-HHD (left) and CCM2-HHD-E290R (right). The plots show a major species with a molecular weight consistent with the monomer (10.9 kDa, 95% confidence intervals: 9.3, 12.6 kDa). The *y*-axis denotes the anisotropy of the molecule, which suggests a mostly globular structure with a value of 1.35 (95% confidence interval: 1.25, 1.44). The color scale on the right *y*-axis denotes relative concentration.

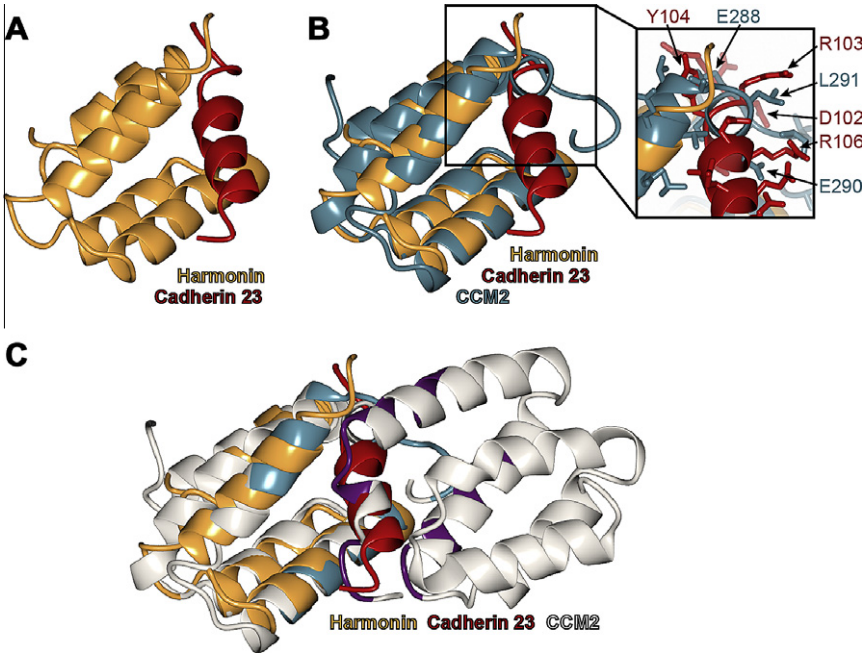

Fig. 5. CCM2 HHD crystallographic dimerization interface is analogous to harmonin–cadherin 23 interface. (A) structure of harmonin N-terminal domain (orange) bound to a cadherin 23 peptide in red (PDB ID: 2KBR) [15]; (B) superposition of CCM2-HHD (teal) and harmonin (orange). Cadherin 23 is shown (red). Exploded view shows specific residues that clash between CCM2-HHD and cadherin 23 in the superposition; (C) superposition of the CCM2-HHD dimer onto harmonin. The cadherin binding site is equivalent to the dimer interface between CCM2 HHD chain A (left, interface residues teal) and chain B (right, interface residues purple).

interface primarily observable under crystallization conditions. These studies do not, however, preclude the potential that other regions of CCM2 or CCM2 binding partners could facilitate formation of this dimerization interface.

3.8. The crystallographic CCM2 HHD dimerization interface resembles the harmonin–cadherin 23 binding site

The CCM2 HHD is structurally similar to the N-terminal domain of the Usher syndrome protein harmonin (Fig. 2D). Harmonin binds directly to the cell adhesion protein cadherin 23 via two domains: its N-terminal domain and a PDZ domain. The structural basis for the harmonin N-terminal domain binding to cadherin 23 has been determined by NMR spectroscopy [15] (Fig. 5A), so we compared this mode of binding to the crystallographically-observed CCM2 HHD dimer. We found that the CCM2 HHD dimer interface occupies a similar location to that observed for the harmonin interaction with cadherin 23 (Fig. 5B and C). Although we did not observe direct interaction between CCM2-HHD and cadherin 23 (data not shown) we suggest that the equivalent surface in CCM2 HHD could potentially mediate other protein–protein interactions.

4. Discussion

Understanding the function and role of proteins associated with cerebral cavernous malformations has recently become an area of intense interest, as KRIT1, CCM2, and CCM3 have been found to be involved in diverse signaling pathways. These include regulation of integrin activation, degradation of Rho-family GTPases and receptor tyrosine kinases, stabilization of VEGFR2, interactions with MAP and sterile-20 kinases, and TrkA signaling. The discovery of new regions within these proteins that can provide a functional basis for understanding their signaling pathways could therefore allow for significant further studies. Previously, we discovered that CCM3 contains an N-terminal dimerization domain of a novel fold, and a C-terminal focal adhesion targeting (FAT)-homology domain [9], allowing us to discover interesting new functions and roles for CCM3 [22,23]. Likewise, the current study provides the first molecular level description of CCM2: the discovery of a previously uncharacterized folded domain at its C-terminus that we term the CCM2 harmonin homology domain (HHD). Interestingly we observe two conformations for the CCM2 HHD in our structure.

The similarities between the CCM2 HHD dimerization interface and the harmonin–cadherin 23 interface are interesting. The non-overlapping interactions of the harmonin N-terminal and PDZ domains with cadherin 23 are both of moderate affinity (K_D of approximately 10–20 μM). Together, however, these facilitate a tight harmonin–cadherin 23 complex [15]. Similarly, CCM2 could also potentially utilize bidentate moderate affinity interactions to specific partners, perhaps via both the PTB and HHD domains.

Therefore, the discovery of the HHD provides an exciting new level of understanding to these important proteins and will likely spur new functional analyses of CCM2, its binding partners, and their function.

Acknowledgements

We thank V. Schirf, W. Min, B. Turk, H.J. Lou, K. Draheim, A. Stiegler, W. Liu, N. Alicea-Velázquez, B.H. Ha, J. Chacon, D. Calderwood, J. Ferrullo, and beamlines X25, X29, and NECAT. Grants from NSF (O.S.F.), AHA (X.L.), NIH CA054174, RR022200 (B.D.), and NSF TG-MCB070038 (B.D.). T.J.B. funded by the NIH.

Appendix A. Supplementary data

Supplementary data associated with this article can be found, in the online version, at http://dx.doi.org/10.1016/j.febslet.2012.12.011.

References

[1] Cavalcanti, D.D., Kalani, M.Y., Martirosyan, N.L., Eales, J., Spetzler, R.F. and Preul, M.C. (2012) Cerebral cavernous malformations: from genes to proteins to disease. J. Neurosurg. 116, 122–132.
[2] Akers, A.L., Johnson, E., Steinberg, G.K., Zabramski, J.M. and Marchuk, D.A. (2009) Biallelic somatic and germline mutations in cerebral cavernous malformations (CCMs): evidence for a two-hit mechanism of CCM pathogenesis. Hum. Mol. Genet. 18, 919–930.
[3] Pagenstecher, A., Stahl, S., Sure, U. and Felbor, U. (2009) A two-hit mechanism causes cerebral cavernous malformations: complete inactivation of CCM1, CCM2 or CCM3 in affected endothelial cells. Hum. Mol. Genet. 18, 911–918.
[4] Boulday, G., Blecon, A., Petit, N., Chareyre, F., Garcia, L.A., Niwa-Kawakita, M., Giovannini, M. and Tournier-Lasserve, E. (2009) Tissue-specific conditional CCM2 knockout mice establish the essential role of endothelial CCM2 in angiogenesis: implications for human cerebral cavernous malformations. Dis. Model. Mech. 2, 168–177.
[5] Whitehead, K.J. et al. (2009) The cerebral cavernous malformation signaling pathway promotes vascular integrity via Rho GTPases. Nat. Med. 15, 177–184.
[6] Liquori, C.L. et al. (2003) Mutations in a gene encoding a novel protein containing a phosphotyrosine-binding domain cause type 2 cerebral cavernous malformations. Am. J. Hum. Genet. 73, 1459–1464.
[7] Stahl, S. et al. (2008) Novel CCM1, CCM2, and CCM3 mutations in patients with cerebral cavernous malformations: in-frame deletion in CCM2 prevents formation of a CCM1/CCM2/CCM3 protein complex. Hum. Mutat. 29, 709–717.
[8] Zawistowski, J.S., Stalheim, L., Uhlik, M.T., Abell, A.N., Ancrile, B.B., Johnson, G.L. and Marchuk, D.A. (2005) CCM1 and CCM2 protein interactions in cell signaling: implications for cerebral cavernous malformations pathogenesis. Hum. Mol. Genet. 14, 2521–2531.
[9] Li, X., Zhang, R., Zhang, H., He, Y., Ji, W., Min, W. and Boggon, T.J. (2010) Crystal structure of CCM3, a cerebral cavernous malformation protein critical for vascular integrity. J. Biol. Chem. 285, 24099–24107.
[10] Zhou, X., Izumi, Y., Burg, M.B. and Ferraris, J.D. (2011) Rac1/osmosensing scaffold for MEKK3 contributes via phospholipase C-gamma1 to activation of the osmoprotective transcription factor NFAT5. Proc. Natl. Acad. Sci. USA 108, 12155–12160.
[11] Uhlik, M.T. et al. (2003) Rac-MEKK3-MKK3 scaffolding for p38 MAPK activation during hyperosmotic shock. Nat. Cell. Biol. 5, 1104–1110.
[12] Crose, L.E., Hilder, T.L., Sciaky, N. and Johnson, G.L. (2009) Cerebral cavernous malformation 2 protein promotes smad ubiquitin regulatory factor 1-mediated RhoA degradation in endothelial cells. J. Biol. Chem. 284, 13301–13305.
[13] Harel, L. et al. (2009) CCM2 mediates death signaling by the TrkA receptor tyrosine kinase. Neuron 63, 585–591.
[14] Yan, J., Pan, L., Chen, X., Wu, L. and Zhang, M. (2010) The structure of the harmonin/sans complex reveals an unexpected interaction mode of the two Usher syndrome proteins. Proc. Natl. Acad. Sci. USA 107, 4040–4045.
[15] Pan, L., Yan, J., Wu, L. and Zhang, M. (2009) Assembling stable hair cell tip link complex via multidentate interactions between harmonin and cadherin 23. Proc. Natl. Acad. Sci. USA 106, 5575–5580.
[16] Kean, M.J. et al. (2011) Structure–function analysis of core STRIPAK proteins: a signaling complex implicated in golgi polarization. J. Biol. Chem. 286, 25065–25075.
[17] Enkhbayar, P., Hikichi, K., Osaki, M., Kretsinger, R.H. and Matsushima, N. (2006) 3(10)-Helices in proteins are parahelices. Proteins 64, 691–699.
[18] Dyer, D.H., Lovell, S., Thoden, J.B., Holden, H.M., Rayment, I. and Lan, Q. (2003) The structural determination of an insect sterol carrier protein-2 with a ligand-bound C16 fatty acid at 1.35-A resolution. J. Biol. Chem. 278, 39085–39091.
[19] Vieira-Pires, R.S. and Morais-Cabral, J.H. (2010) 3(10) Helices in channels and other membrane proteins. J. Gen. Physiol. 136, 585–592.
[20] McNicholas, S., Potterton, E., Wilson, K.S. and Noble, M.E. (2011) Presenting your structures: the CCP4mg molecular-graphics software. Acta Crystallogr. D: Biol. Crystallogr. 67, 386–394.
[21] Lawrence, M.C. and Colman, P.M. (1993) Shape complementarity at protein/protein interfaces. J. Mol. Biol. 234, 946–950.
[22] Li, X., Ji, W., Zhang, R., Folta-Stogniew, E., Min, W. and Boggon, T.J. (2011) Molecular recognition of LD motifs by the FAT-homology domain of cerebral cavernous malformation 3 (CCM3). J. Biol. Chem. 286, 26138–26147.
[23] He, Y., Zhang, H., Yu, L., Gunel, M., Boggon, T.J., Chen, H. and Min, W. (2010) Stabilization of VEGFR2 signaling by cerebral cavernous malformation 3 is critical for vascular development. Sci. Signal. 3, ra26.